Analytical Methods

PAPER

View Article Online
View Journal | View Issue

Cite this: *Anal. Methods*, 2015, 7, 2693

An electrochemical sensor for selective determination of sulfamethoxazole in surface water using a molecularly imprinted polymer modified BDD electrode†

Yang Zhao,[a] Fang Yuan,[a] Xie Quan,*[a] Hongtao Yu,[a] Shuo Chen,[a] Huimin Zhao,[a] Zhaoyang Liu[b] and Nidal Hilal[b]

Received 23rd December 2014
Accepted 3rd February 2015

DOI: 10.1039/c4ay03055a

www.rsc.org/methods

This study presents a new electrochemical sensor based on a molecularly imprinted polymer (MIP) modified boron doped diamond (BDD) electrode (MIP/BDD electrode) for the quantitative determination of sulfamethoxazole (SMX). This MIP/BDD electrode is prepared by *in situ* electro-polymerization of pyrrole (Py) on the BDD electrode in the presence of SMX. This sensor based on the MIP/BDD electrode performs a linear response for SMX from 0.1–100 μM with a limit of detection of 24.1 nM ($S/N = 3$) and a highly reproducible response (2.32%). The detection of SMX in surface water samples spiked at different concentration levels performs satisfactorily at a recovery of 96.0–106.2%. Furthermore, this sensor exhibits a superior selectivity to recognize SMX molecules even compared with other structural analogues (SDM, SD and SIZ). This high-selectivity determination originates from the imprinted sites of the MIP film which have the advantages of appropriate cavity size and homologous functional groups for the specific recognition of SMX molecules. This specially designed sensor offers a simple, selective, sensitive, reliable, stable and environmentally friendly approach for SMX determination, providing a responsible strategy for effective SMX analysis in environmental water.

Introduction

Antibiotics and synthetic antimicrobial agents are widely used in the treatment of human infections, as well as in agriculture, animal husbandry as veterinary drugs and growth promoters.[1–4] These chemical compounds are inevitably discharged into the environment mainly by disposal of domestic sewage, expired medicines, urine and faeces in non-metabolized forms or coupling with polar molecules.[5–7] The residue of the antibiotics and synthetic antimicrobial agents in the environment has resulted in the bacterial resistance, which could seriously affect the human health and ecological balance. It has been regarded as one of the major threats to public health on a worldwide scale by the World Health Organization.[8–11] Among these antimicrobial agents, sulfamethoxazole (SMX, 4-amino-*N*-(5-methyl-3-isoxazolyl) benzene sulphonamide) is one of the most typical antimicrobial agents due to its common use,[12,13] which is reported with acute toxicity, chronic toxicity,[14] mutagenic activity[15] and even potential endocrine disruption.[16] Therefore, the development of a selectivity assay for SMX with high sensitivity is significant in the supervision and management of its discharge.

The traditional methods for SMX detection, such as bioanalysis, immunoassays and chemical–physical methods, are limited by time-consuming, nonspecific, expensive equipment, tedious sample pre-treatment and use of organic solvents.[17–25] In comparison with the traditional methods, electrochemical sensors based on various functional electrodes possess the following advantages: rapid response, low cost, simplicity and environmental friendliness.[26,27] In the electrochemical detection processes, the accuracy and efficiency are dependent on the electrode materials. A boron doped diamond (BDD) electrode is a kind of environmentally friendly carbon electrode with significant advantages,[28,29] such as wide electrochemical working potential window, high mechanical strength and corrosion resistance, high resistance to deactivation and long term response stability, and low and stable background current. BDD has been reported to simultaneously detect SMX and trimethoprim (TMP, with a quite different structure from SMX) based on the mechanism of electrochemical mineralization.[30] However, the selectivity based on the mineralization mechanism is influenced by the presence of other sulphonamides which contain the same parent structure as SMX (Fig. S1†), such

---

[a] *Key Laboratory of Industrial Ecology and Environmental Engineering (Ministry of Education, China), School of Environmental Science and Technology, Dalian University of Technology, Dalian 116024, China*

[b] *Qatar Environment and Energy Research Institute, Qatar Foundation, PO Box 5825, Doha, Qatar*

† Electronic supplementary information (ESI) available. See DOI: 10.1039/c4ay03055a

as sulfadimethoxine (SDM), sulfadiazine (SD) and sulfafurazole (SIZ). They exhibit analogous electrochemical oxidation behaviours which result in the overlapped oxidation peak potentials.[31] Hence, it is important to develop a rapid and environmentally friendly electrochemical sensor for the selective and sensitive determination of SMX with a low LOD.

In recent years, molecularly imprinted polymers (MIPs) have been investigated as selective sorbent materials in sample pretreatment due to their excellent selectivity for the template molecule.[32–34] In the fabrication process of MIPs, the spatial structure of imprinted cavities, matching with template molecules, is formed by the interaction between the template molecule and functional monomer. The imprinted cavities can selectively recognize the template molecules through the “antigen–antibody” mechanism which can distinctly improve the selectivity for the target molecule.[35] The conductive MIP has been widely used to improve the sensitivity and selectivity performance of sensors.[36,37] The conductive MIP provides a number of imprinted cavities and enhances the ability of electron transfer from the binding sites to the electrode surface.[38,39] Therefore, the selectivity and sensitivity of electrochemical sensors based on the BDD electrode could be significantly improved by the conductive MIP modified processes, which has not been reported until now.

The present study aims to develop a reliable and stable electrochemical sensor based on the MIP/BDD electrode for selective and sensitive determination of SMX in surface water. This MIP/BDD electrode is fabricated by *in situ* electro-polymerization of pyrrole (Py) in the presence of SMX. The detection condition is optimized for SMX detection. The selectivity of this sensor for SMX is investigated with other sulphonamides as interferents. The “antigen–antibody” mechanism of this SMX detection ensures the high selectivity of the detection. Furthermore, the electrochemical sensor based on the MIP/BDD electrode is performed for the determination of SMX in surface water spiked at different concentration levels.

Experimental

Preparation of BDD electrodes

A microwave plasma chemical vapor deposition (MPCVD) process is used to deposit BDD on the Si (111) substrate. A mixture of CH_4, diluted B_2H_6 (by H_2) and H_2 is used as the source gas, wherein the concentrations of CH_4 and B_2H_6 are 0.5–2.0 vt% and 0.05–0.2 vt%, respectively. During the deposition process, the total flow rate, the pressure of the chamber, substrate temperature and deposition duration are 100 sccm, 6 kPa, 480 °C and 8 h, respectively.

Modification of the BDD electrode by *in situ* electro-polymerization of MIPs

The BDD electrode is cleaned by ultrasonic treatment first in ultrapure water, then in the solution mixed with isopropyl alcohol and acetonitrile (1 : 1 v/v). The electrode is dried by argon gas before electro-polymerization. The MIP film is obtained by electro-polymerizing Py on the surface of the BDD electrode *via* a cyclic voltammetry (CV) process (operating parameters:[40] from −0.6 V to +1.8 V, 50 mV s^{-1}, phosphate buffer solution (PBS)). In the PBS, SMX acts as a template molecule, Py acts as a functional monomer and cross-linking agent. In order to elute the template molecule (SMX) from the MIP, the MIP/BDD electrode is immersed in 1.0 M NaOH and stirred for 60 min. The control experiment (non-imprinted polymer modified electrode, NIP/BDD) is prepared under the same experimental conditions without the template molecule SMX.

Characterization

The general morphology of the MIP/BDD electrode is characterized by field emission scanning electron microscopy (FESEM, Hitachi S-4800). The Raman spectrum is obtained from a Renishaw Micro-Raman System 2000 Spectrometer operated at He–Ne laser excitation (wavelengths 623.8 nm and laser power 35 mW) with a beam spot size of about 2 μm. X-ray diffraction (XRD) is used to identify the crystal of the MIP/BDD electrode.

Electrochemical experiments are performed on an electrochemical workstation (CHI 650B) at room temperature in a conventional three-electrode electrochemical cell (5 cm in depth and 3 cm in diameter). The MIP/BDD electrode acts as the working electrode with a geometric area of 1 cm^2. A platinum electrode and a saturated calomel electrode (SCE) are used as the control and reference electrode, respectively. To characterize the electrochemical properties of the electrodes, CV experiments are performed in the voltage range of 0.25–0.5 V at a scan rate of 50 mV s^{-1} in the solution of 0.1 M KCl containing 1 mM $Fe(CN)_6^{3-/4-}$.

Quantitative analysis of SMX

The determination of SMX is performed in PBS (10 mL) using square wave voltammetry (SWV) from 0.55 to 0.97 V. The amplitude, frequency and increment of potential are 25 mV, 10 Hz and 4 mV, respectively. The peak current is recorded as I_{peak} at 0.88 V. A steady blank current (I_{blank}) is recorded under the same conditions without SMX in PBS. The value of I_{blank} minus I_{peak} is calculated and defined as the response current (ΔI). After the experiment, the electrode is immersed in 1.0 M NaOH solution and stirred for 60 min to elute the SMX from the imprinting sites on the surface of the electrode.

The surface water is obtained from a lake in Dalian, China (Table S1†). Prior to the sample analysis, the lake water sample is pre-treated by the following processes. First, the lake water sample is filtered by suction filtration (0.2 μm) to exclude the effect caused by suspended particles and microorganisms. Then, the filtered water sample is used to prepare PBS (pH 7.0). The pre-treated water sample is kept at 4 °C.

Results and discussion

Modification of the BDD electrode by *in situ* electro-polymerized MIPs

The MIP/BDD electrode is obtained by *in situ* electro-polymerization on the surface of the BDD electrode using CV in a potential range between −0.6 V and +1.8 V (Fig. 1). The oxidation peak at about 1.03 V is clearly observed in the process of electro-polymerization and visibly disappears in subsequent cycles. It suggests that the Py molecules are successfully electro-polymerized on the surface of BDD. The electro-polymerization of the SMX imprinting polypyrrole (Ppy) film process is described as follows (Scheme 1).

Py molecules lose an electron to form cation radicals on a BDD anode. Then cation radicals collide with each other to form a Ppy dimer which can subsequently combine with other cation radicals in the system to form the Ppy film. SMX anions diffuse into BDD under the common action of an electric field and electrostatic interactions with Py cation radicals. The N atoms of Ppy can act as not only an electron receptor but also an electron donor to form non-covalent bonds with SMX to form the SMX MIP film.[41] And in the MIP film, the transfer of the π electron in the conjugated structure of Ppy makes the polymer film conductive in the electric field. Then, the free Py molecules on the MIP/BDD electrode are removed by PBS (pH 7.5), and the template molecules are removed by breaking the hydrogen bonds in the elution step.

Effect of pH, template concentration, cycles and monomer concentration on MIP electro-polymerization

In order to obtain the optimal conditions of electro-polymerization of MIPs on the BDD electrode, an orthogonal experiment is designed with 4 influence factors which are pH, template concentration (c_{SMX}), electro-polymerization cycles and monomer concentration (c_{Py}), and 4 levels are set for each influence factor (Table S2†). The response currents (ΔI) to 100 μM SMX measured by the prepared MIP/BDD electrodes are used to evaluate the performance of each MIP/BDD electrode. The results of the orthogonal experiment (L16 (4^4)) are investigated by the range analysis (Table S3†). It shows that the effect of the factors on ΔI is in the order of c_{SMX}, c_{Py}, pH, cycles and the optimized conditions of the electro-polymerization. The results are analyzed as follows (shown in Fig. S2†).

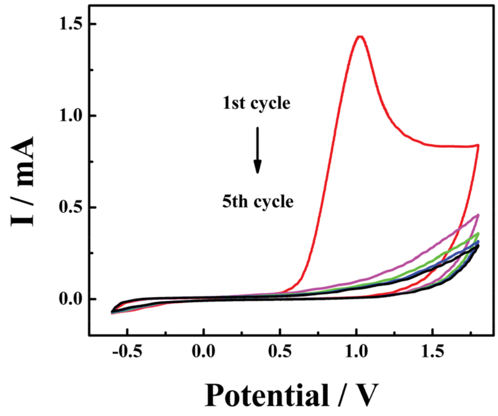

Fig. 1 Cyclic voltammogram for *in situ* electro-polymerization of Py (40 mM) on BDD in PBS (pH 7.5) containing 20 mM SMX (scan rate 50 mV s^{-1}, 5 cycles).

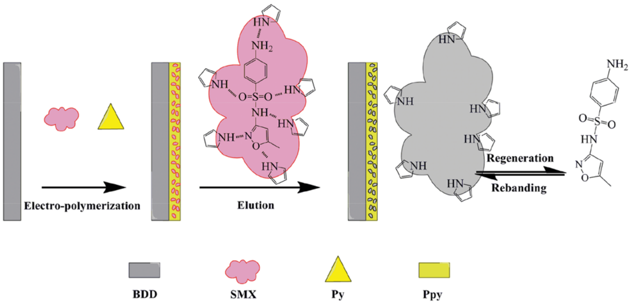

Scheme 1 Schematic diagram for fabrication of the MIP/BDD electrode.

The quantity of the imprinted sites increases with the increase of SMX concentration. On the other hand, the intact conjunction cavities in Ppy fail to form in the electro-polymerization reaction with high concentration SMX due to the competition effect of excessive SMX. The experimental results prove that the ΔI to c_{SMX} on the MIP/BDD electrode is dramatically reduced when the c_{SMX} is over 20 mM. The optimization of the concentration of the functional monomer Py and the CV cycles are performed in a series of experiments. The thickness of the MIP film, as well as the imprinted sites, increases with the c_{Py} and CV cycles. Meanwhile, the sites are also covered by the newly formed Ppy. The ΔI reaches the maximum value under the conditions of 40 mM Py and 5 cycles. As an amphoteric compound, the existing form of SMX depends on the pH of the system (Scheme 2). SMX dissociates into negatively charged anions when the pH of PBS is higher than pK_{a2} (5.6).[42] Therefore, different PBS solutions (pH 7, 7.5, 8 and 9) are used as the electrolyte solution in the electro-polymerization, in which SMX anions can diffuse into the anode in the electric field. And the largest ΔI to SMX is obtained at pH 7.5. Summing up the above, 20 mM SMX, 40 mM Py, pH 7.5 and 5 cycles are chosen as the optimum conditions for the following *in situ* electro-polymerization experiment.

Characterization of the MIP/BDD electrode

The intensity ratio of sp^3 and sp^2 hybridization peaks and the full width at half maximum (FWHM) of the sp^3 hybridization peak are used to evaluate the BDD material. As shown in Fig. 2, there are sharp and narrow sp^3 hybridization peaks at 1332 cm^{-1} in the Raman spectrum of all the electrodes. And there are broad sp^2 hybridization peaks in the range of 1400–1650 cm^{-1} in the Raman spectrum of MIP/BDD, non-eluted MIP/BDD and NIP/BDD. It is caused by the conjugate structure of the Ppy film which is composed of a large number of sp^2

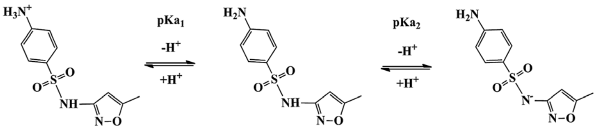

Scheme 2 Schematic diagram for equilibrium of SMX (pK_1 = 1.7 and pK_2 = 5.6).

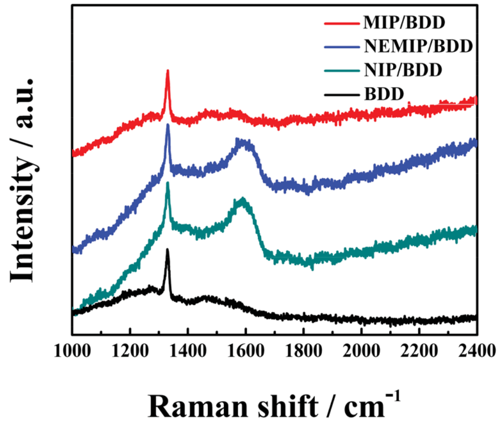

Fig. 2 Raman spectrum of different electrodes.

hybridized carbon atoms. It can be speculated that the Ppy film is successfully polymerized on the BDD surface. The strong sp^2 hybridization peak in non-eluted MIP/BDD (NEMIP/BDD) and NIP/BDD may be caused by residual Py or SMX molecules.

The morphology of MIP/BDD and BDD is characterized by FESEM. As shown in Fig. 3(a) and (b), BDD is continuous and uniform, and the size of the diamond grain is in the range of 0.2 to 1 μm. In Fig. 3(c) and (d), the BDD particle is uninjured in the process of electro-polymerization. Compared with BDD in Fig. 3(a) and (b), the details (stripe and etching spots) on the surface of the BDD particle are covered by the MIP film, and bright edge and wrinkles are shown on the MIP film. BDD is completely covered with a layer of continuous MIP film. In addition, the MIP film on the BDD edge is observed to be thicker than that on the surface. Due to the smaller curvature radius of the edge, the charge density and the electro-polymerization reaction here are stronger which results in a thicker MIP film.

XRD analysis is performed to investigate the BDD crystal, which is shown in Fig. S3.† Compared with the standard XRD spectrogram of diamond (PCPDF card no. 65-0537), the diffraction peaks at 44° and 75.4° correspond to (111) and (220) lattice planes of diamond, respectively. The stronger diffraction peak at 44° proves that the diamond (111) is the dominant growth direction in BDD. The BDD crystal structure of all the electrodes is not influenced by the electro-polymerization process, and the MIP film consisting of Ppy or Ppy/SMX is weakly bonded as non-crystalline polymers. All the above points suggest that the structure of BDD is not changed by the process of *in situ* electro-polymerization.

The electrochemical performance of the MIP/BDD electrode is tested by the CV method. Detection based on the MIP/BDD electrodes is a signal acquisition process of currents produced by specific binding between the MIP and target molecule SMX, which can interfere with the electron transfer of the redox reaction on the bare BDD electrode. So the complete coverage by the MIP film on the BDD electrode is significant to make sure that the electrical signal is completely acquired from specific binding. So the redox activity of the electrodes is investigated by CV of $Fe(CN)_6^{3-/4-}$. As shown in Fig. 4, compared with that on the BDD electrode, the reversible redox peaks of $Fe(CN)_6^{3-/4-}$ on MIP/BDD and NIP/BDD electrodes disappeared. It demonstrates that no redox process occurred, so the BDD electrode is completely covered by the MIP film. It is also consistent with the characterization results of the Raman spectrum and FESEM.

Detection of SMX

In order to investigate the influence of pH in the process, three kinds of pH (faintly acid (pH 6.0), neutral (pH 7.0) and alkalescence (pH 9.0)) are set for the determination of SMX. As shown in Fig. S4,† the Δ*I* in PBS (pH 7.0) is almost twice that in PBS (pH 6.0 and 9.0). Therefore, PBS (pH 7.0) is chosen in the following detection experiments. As shown in Fig. 5(a), the response current on the MIP/BDD electrode gradually increases with the increase of the SMX concentration. The results are in conformity with the linear relationship for the concentration range 0.1–100 μM. The calibration curve is shown in Fig. 5(b) with a correlation coefficient of 0.9997. The linear regression equation is as follows:

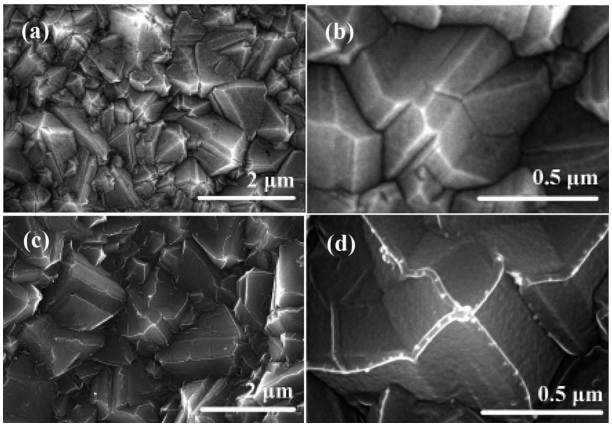

Fig. 3 FESEM images of (a and b) BDD and (c and d) MIP/BDD.

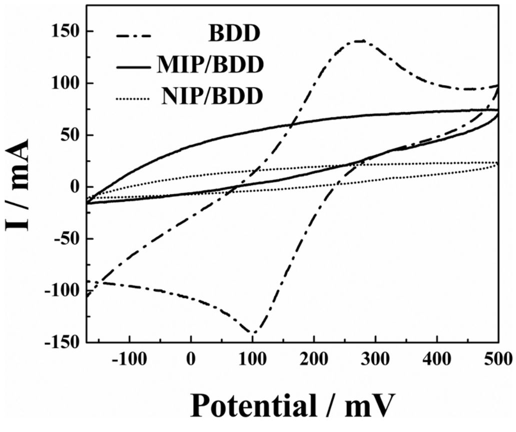

Fig. 4 CV responses of 1.0 mM $Fe(CN)_6^{3-/4-}$ in 0.1 M KCl at a scan rate of 50 mV s^{-1} on MIP/BDD, NIP/BDD and BDD electrodes.

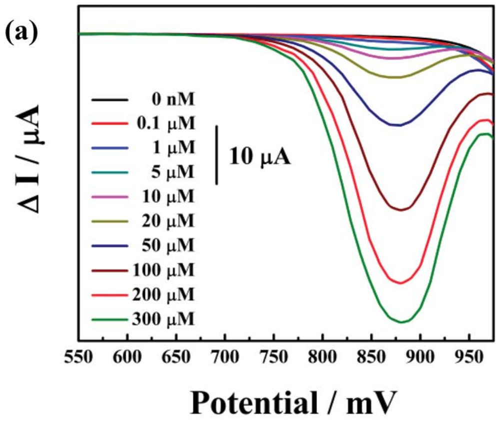

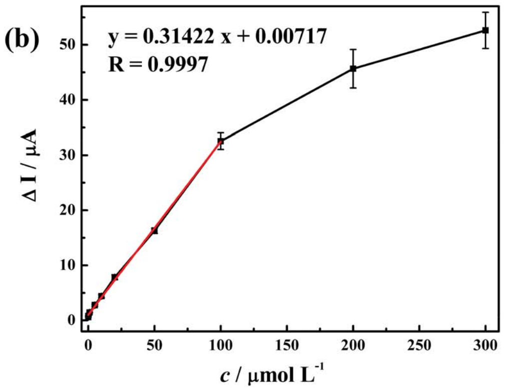

Fig. 5 SWV responses (a) and calibration curves (b) of varying concentrations at the MIP/BDD electrode in PBS solution (pH 7.0) ($n = 6$).

$$y = 0.31422x + 0.00717,\ R = 0.9997,\ n = 6$$

The LOD of this assay is calculated to be 24.1 nM ($S/N = 3$), which is much lower than other electrochemical detection methods (Table 1).

The reliability of this sensor is evaluated by repetitive experiments ($n = 6$). The RSD is 2.32% for the ΔI measured in 50 μM SMX standard solution which demonstrates the reliability of the assay. After 30 days (in a glass desiccator at room temperature), the value of ΔI is approximately 96.7% of the original value. It verifies the excellent stability of the MIP/BDD electrode.

Table 1 Comparison of different methods

Technique	LOD	Description	References
Immunoassay	10 ng mL^{-1}		18
Spectrophotometric	0.34 μg mL^{-1}		19
Capillary electrophoresis	0.1 μmol L^{-1}		20
HPLC	80 ng mL^{-1}		24
Electrochemistry	65.1 nmol L^{-1}	BDD	30
	24.1 nmol L^{-1}	MIP/BDD	This study

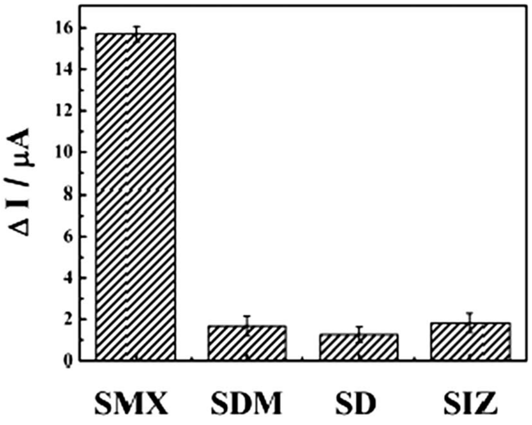

Fig. 6 SWV responses in the presence of SMX (50 μM), SDM (500 μM), SD (500 μM) and SIZ (500 μM) at the MIP/BDD electrode in PBS solution (pH 7.0), respectively.

Specificity of the sensor

To evaluate the selectivity of this electrochemical sensor, the anti-interference experiments are performed with three kinds of structurally similar sulphonamides (SDM, SD and SIZ) as interferents. In a typical experiment, the electrochemical process based on the MIP/BDD electrode is conducted with 50 μM SMX, 500 μM SD, 500 μM SIZ and 500 μM SDM in PBS (pH 7.0), respectively. As shown in Fig. 6, the ΔI for SMX (50 μM) is 15.71 μA, while it is 1.67 μA for SDM (500 μM), 1.26 μA for SD (500 μM) and 1.82 μA for SIZ (500 μM). It is obvious that the sensor exhibits good selectivity which is attributed to the specificity of MIPs toward SMX based on the "antigen–antibody" mechanism. The imprinted cavities with appropriate size provide homologous functional groups for the specific recognition of SMX molecules.

Detection of SMX in lake water samples

In order to evaluate the feasibility of its potential in the real aquatic environment, this electrochemical sensor based on MIP/BDD is applied to detect SMX in lake water samples. SMX in the pre-treated lake water sample is detected by this sensor. It is found that the SMX content in the lake water is too low to be detected by this sensor. Hence, SMX in the samples spiked at three different concentrations is detected. The analytical results for the samples spiked with 0.5–30 μM of standard SMX are given in Table 2. The recovery is in the range of 96.0–106.2%, which indicates that the developed assay can be performed for the accurate determination of SMX in real samples.

Table 2 Recoveries of SMX spiked from lake water samples

Sample	Standard value of SMX (μM)	Found (μM)	Recovery (%)	RSD (%, $n = 5$)
Lake water	0.5	0.48	96.0	2.65
	5.0	5.31	106.2	1.29
	30.0	31.28	104.3	3.94

Conclusions

A new electrochemical sensor based on a MIP/BDD electrode is developed for selective and sensitive electrochemical detection of SMX in surface water. This sensor based on the MIP/BDD electrode displays a good reliability (2.32%), excellent recognition selectivity and low LOD (24.1 nM). More importantly, this sensor performs a high recovery (96.0–106.2%) for the spiked detection of SMX in real water samples. The above advantages may be attributed to the imprinted sites on the surface of the MIP/BDD electrode. This electrochemical sensor for selective, sensitive, reliable and stable detection of SMX in surface water provides a firm basis for the supervision and management of SMX in the environment.

Acknowledgements

This work was supported by the National Basic Research Program of China (2011CB936002).

Notes and references

1 B. H. Sorensen, S. N. Nielsen, P. F. Lanzky, F. Ingerslev, H. H. Liitzhofl and S. E. Jorgensen, *Chemosphere*, 1998, **36**, 357.
2 K. Kümmerer, *Chemosphere*, 2009, **75**, 417.
3 B. Petrie, R. Barden and B. Kasprzyk-Hordern, *Water Res.*, DOI: 10.1016/j.watres.2014.08.053, in press
4 N. Kemper, *Ecol. Indic.*, 2008, **8**, 1.
5 X. S. Miao, F. Bishay, M. Chen and C. D. Metcalfe, *Environ. Sci. Technol.*, 2004, **38**, 3533.
6 C. Moschet, C. Götz, P. Longreìe, J. Hollender and H. Singer, *Environ. Sci. Technol.*, 2013, **47**, 7028.
7 A. Rodayan, R. Roy and V. Yargeau, *J. Hazard. Mater.*, 2010, **177**, 237.
8 K. Oberlé, M. J. Capdeville, T. Berthe, H. Budzinski and F. Petit, *Environ. Sci. Technol.*, 2012, **46**, 1859.
9 M. A. Gilliver, M. Bennett, M. Begon, S. M. Hazel and C. A. Hart, *Nature*, 1999, **401**, 233.
10 J. C. Underwood, R. W. Harvey, D. W. Metge, D. A. Repert, L. K. Baumgartner, R. L. Smith, T. M. Roane and L. B. Barber, *Environ. Sci. Technol.*, 2011, **45**, 3096.
11 A. El-Ghenymy, P. L. Cabot, F. Centellas, J. A. Garrido, R. M. Rodríguez, C. Arias and E. Brillas, *Electrochim. Acta*, 2013, **90**, 254.
12 S. Ding, J. Niu and Y. Bao, *Environ. Sci. Technol.*, 2013, **262**, 812.
13 H. Lin, J. F. Niu, J. L. Xu, Y. Li and Y. H. Pan, *Electrochim. Acta*, 2013, **97**, 167.
14 S. J. Park and K. Choi, *Ecotoxicology*, 2008, **17**, 526.
15 M. Isidori, M. Lavorgna, A. Nardelli, L. Pascarella and A. Parrella, *Sci. Total Environ.*, 2008, **346**, 87.
16 L. B. Barber, S. H. Keefe, D. R. Leblanc, P. M. Bradley, F. H. Chapelle, M. T. Meyer, K. A. Loftin, D. W. Kolpin and F. Rubio, *Environ. Sci. Technol.*, 2009, **43**, 4843.
17 W. Haasnoot, M. B. Ploum, U. Lamminmäki, M. Swanenburg and H. V. Rhijn, *Anal. Chim. Acta*, 2005, **552**, 87–95.
18 Z. H. Wang, R. C. Beier, Y. J. Sheng, S. X. Zhang, W. X. Jiang, Z. P. Wang, J. Wang and J. Z. Shen, *Anal. Bioanal. Chem.*, 2013, **405**, 4027.
19 L. L. Martínez, P. L. López-de-Alba, L. M. de-León-Rodríguez and M. L. Yepez-Murrieta, *J. Pharm. Biomed. Anal.*, 2002, **30**, 77.
20 T. Y. You, X. R. Yang and E. K. Wang, *Analyst*, 1998, **123**, 2357.
21 J. J. BerzasNevado, G. CastañedaPeñalvo and F. J. Guzmán Bernardo, *Anal. Chim. Acta*, 2001, **442**, 241.
22 A. G. Trovó, R. F. Nogueira, A. Agüera, C. Sirtori and A. R. Fernández-Alba, *Chemosphere*, 2009, **77**, 1292.
23 D. H. Shewiyo, E. Kaale, P. G. Risha, B. Dejaegher, J. S. Verbeke and Y. V. Heyden, *J. Chromatogr. A*, 2009, **1216**, 7102.
24 F. C. de Paula, A. C. de Pietro and Q. B. Cass, *J. Chromatogr. A*, 2008, **1189**, 221.
25 I. Cesarino, V. Cesarino and M. R. Lanza, *Sens. Actuators, B*, 2013, **188**, 1293.
26 C. Gao, Z. Guo, J. H. Liu and X. J. Huang, *Nanoscale*, 2012, **4**, 1948.
27 Y. Y. Shao, J. Wang, H. Wu, J. Liu, I. A. Aksay and Y. H. Lin, *Electroanalysis*, 2010, **22**, 1027.
28 G. W. Muna, N. Tasheva and G. M. Swain, *Environ. Sci. Technol.*, 2004, **38**, 3674.
29 A. Kirste, G. Schnakenburg, F. Stecker, A. Fischer and S. R. Waldvogel, *Angew. Chem., Int. Ed.*, 2010, **49**, 971.
30 L. S. Andrade, R. C. Filho, Q. B. Cass and O. F. Filho, *Anal. Methods*, 2010, **2**, 402.
31 C. D. Souza, O. C. Braga, I. C. Vieira and A. Spinelli, *Sens. Actuators, B*, 2008, **135**, 66.
32 V. Suryanarayanan, C. Wu and K. Ho, *Electroanalysis*, 2010, **22**, 1795–1811.
33 M. Valtchev, B. S. Palm, M. Schiller and U. Steinfeld, *J. Hazard. Mater.*, 2009, **170**, 722.
34 X. J. Liu, C. B. Ouyang, R. Zhao, D. H. Shangguan, Y. Chen and G. Q. Liu, *Anal. Chim. Acta*, 2006, **571**, 23.
35 J. Q. Liu and G. Wulff, *Angew. Chem., Int. Ed.*, 2004, **43**, 1287.
36 H. da Silva, J. G. Pacheco, J. M. C. S. Magalhães, S. Viswanathan and C. D. Matos, *Biosens. Bioelectron.*, 2014, **52**, 56.
37 M. Zhong, Y. Teng, S. F. Pang, L. Q. Yan and X. W. Kan, *Biosens. Bioelectron.*, 2015, **64**, 212.
38 P. P. Wang, W. J. Dai, L. Ge, M. Yan, Sh. G. Ge and J. H. Yu, *Analyst*, 2013, **138**, 939.
39 C. G. Xie, H. F. Li, S. Q. Li, J. Wu and Z. P. Zhang, *Anal. Chem.*, 2010, **82**, 241.
40 V. K. Gupta, M. L. Yola, N. Özaltın, N. Atar, Z. Üstündag and L. Uzun, *Electrochim. Acta*, 2013, **112**, 37.
41 A. Turco, S. Corvaglia and E. Mazzotta, *Biosens. Bioelectron.*, 2015, **63**, 240.
42 M. C. Dodd and C. H. Huang, *Environ. Sci. Technol.*, 2004, **38**, 5607.